

New mixed-valence oxides of bismuth: $\text{Bi}_{1-x}\text{Y}_x\text{O}_{1.5+\delta}$ ($x=0.4$)

H. Mizoguchi,^{*,†} K. Ueda,^a H. Kawazoe,^a H. Hosono,^b T. Omata^{c,‡} and S. Fujitsu^d

^a Tokyo Institute of Technology, Research Laboratory of Engineering Materials, Nagatsuta, Midori-ku, Yokohama 226, Japan

^b Institute for Molecular Science, Myodaiji, Okazaki 444, Japan

^c Kanagawa Institute of Technology, Shimo-ogino, Atsugi 243-02, Japan

^d The Shonan Institute of Technology, Tujido-Nishikaigan, Fujisawa 251, Japan

New bismuth mixed-valence compounds $\text{Bi}_{1-x}\text{Y}_x\text{O}_{1.5+\delta}$ ($x=0.4$, $0 < \delta \leq 0.16$) have been synthesized by introducing excess oxygens into an anion-deficient fluorite type crystal $\text{Bi}_{0.6}\text{Y}_{0.4}\text{O}_{1.5}$ by heating at 703 K under high oxygen partial pressure up to 300 atm. Values of δ were determined by iodometric titration and thermogravimetric analysis. A distinct red shift of the absorption edge from 2.7 to *ca.* 1.7 eV was observed on going from $\delta=0$ to 0.16. These compounds showed semiconductive properties with an activation energy of 0.9 eV, ruling out the possibility that the introduction of excess oxygen causes the formation of a single-valence Bi ion. These optical and electrical properties demonstrated the formation of a mixed-valence state between $\text{Bi}^{3+} 6s^2$ and $\text{Bi}^{5+} 6s^0$; gap-narrowing was explained by charge-transfer absorption.

Study of mixed-valence states of cations in solids is an attractive topic¹⁻³ because of the unique optical and electrical properties of such materials, *e.g.*, superconductivity as observed in $\text{Ba}(\text{Pb}_{1-x}\text{Bi}_x)\text{O}_3$ ($x \text{ ca. } 0.25$).⁴ In halide complexes of bismuth ions, the mixed-valence states between Bi^{3+} with $6s^2 6p^0$ electronic configuration and Bi^{5+} with $6s^0 6p^0$ are well known. On the other hand, in solid oxides, few materials containing pentavalent bismuth ion have been synthesized so far.⁵⁻¹⁵ Under ordinary redox conditions, Bi^{3+} is not readily oxidized. However, the formation of Bi^{5+} is often observed in oxides containing alkali- or alkaline-earth cations. Alkali- and alkaline-earth ions enhance effective negative charges on the adjacent oxide ions and the large negative charges enable oxidation of some fraction of Bi^{3+} to Bi^{5+} .

The purpose of the present study is to prepare a new mixed-valence oxide of bismuth containing no alkali- or alkaline-earth metallic cations. Recently, we have synthesized mixed-valence oxides of post-transition-metal ions in which inter-valence charge-transfer absorption from ns^2 to ns^0 appeared, by using the following route.¹⁶ $\text{Bi}_{0.6}\text{Y}_{0.4}\text{O}_{1.5} [(\text{Bi}_2\text{O}_3)_{1-x}(\text{Y}_2\text{O}_3)_x, x=0.4]$ ¹⁷⁻²² was selected as the candidate host material. In the present paper, the preparation of $\text{Bi}_{1-x}\text{Y}_x\text{O}_{1.5+\delta}$ ($x=0.4$) in the region $0 < \delta \leq 0.16$ is reported along with the change in optical absorption spectra as a function of δ . The formation of the mixed-valence state of bismuth was investigated.

It is appropriate to give an explanation for the selection of the host material and on the approach to the synthesis of a mixed-valence material with reference to the crystal structure. All bismuth ions in $(\text{Bi}_2\text{O}_3)_{1-x}(\text{Y}_2\text{O}_3)_x$ ($0.10 \leq x \leq 0.43$) exist as Bi^{3+} . The crystal structure can be described as an anion-deficient fluorite structure, represented as $\text{MX}_{1.5}$, and is derived by introducing anionic vacancies into the fluorite structure, MX_2 (cubic, $Fm\bar{3}m$). The cation is coordinated by eight equivalent anions at 8c sites in the fluorite structure. The polyhedron, $\text{MX}_{8/4}$, shares its edges with twelve adjacent ones. In $\text{Bi}_{1-x}\text{Y}_x\text{O}_{1.5}$ ($x=0.4$), disordered Bi^{3+} or Y^{3+} ions occupy the 4a site at random and are coordinated by six anions and two anionic vacancies. A neutron scattering study indicated that there is a small deviation in the position of the cation from

the 4a site.¹⁹⁻²¹ This material is known to show high oxide ionic conductivity, *ca.* $10^{-3} \text{ S cm}^{-1}$ at 773 K, *via* the anionic vacancies.^{17,18} Kruidhof *et al.* reported for $\text{Bi}_{0.7}\text{Y}_{0.3}\text{O}_{1.5}$ that the mass changes depending on the atmosphere at 673–1073 K.^{23,24} A nitrogen or oxygen atmosphere gave rise to a mass loss or gain, respectively, but no discussion was given as to the origin of the mass changes.

The approach employed in converting the single-valence compound to the mixed-valence state is that the trivalent ions in the solid are expected to be oxidized by introducing excess oxygens into the empty anionic sites (8c), 1/4 of which are vacant initially in the $\text{MX}_{1.5}$ compound. Consequently, the $6s^2$ ions in the vicinity of excess O^{2-} are expected to be oxidized to Bi^{n+} ($n > 3$), if the introduction of excess oxygen into the pre-existing vacant 8c site is performed at relatively low temperatures.

Experimental

$\text{Bi}_{0.6}\text{Y}_{0.4}\text{O}_{1.5+\delta}$ samples as discs were prepared by the following procedure. Bi_2O_3 (99.9%) and Y_2O_3 (99.9%) powders were mixed in an agate mortar and pestle with methanol, and the dried mixture obtained was calcined at 1023 K for 10 h in air. The resulting $\text{Bi}_{0.6}\text{Y}_{0.4}\text{O}_{1.5}$ powder was ground, pelletized and sintered at 1183 K for 10 h in air. In order to control the amount of excess oxygen, δ , the pellets were annealed at 703 K under different atmospheres [N_2 , O_2 or $\text{Ar}-\text{O}_2$ (4:1)] for 5 h. The atmosphere of $\text{Ar}-\text{O}_2$ (4:1) at a pressure of 1500 atm was generated by the use of a hot isostatic press (HIP).

X-Ray powder patterns were obtained with a Rigaku RINT2500 X-ray diffractometer using graphite-monochromated Cu-K α radiation (voltage = 50 kV, current = 200 mA) and Si or CaF_2 was used as the internal standard to determine the lattice constant.

Oxygen contents were determined by iodometric titration and thermogravimetry (TG). TG and differential thermal analysis (DTA) were performed on a Rigaku TAS-200 instrument with alumina powder used as a reference. The heating rate employed was 10 K min^{-1} . Electrical conductivities of polycrystalline discs were measured by the dc two-probe method in the temperature range 400–573 K in air. Diffuse reflectance spectra of powder specimens were measured with a Hitachi U-4000 spectrometer. The reflectance was

[†] Present address: Osaka National Research Institute, AIST, Ikeda, Osaka 563, Japan.

[‡] Present address: Osaka University, Faculty of Engineering, Suita, Osaka 565, Japan.

transformed into absorbance by using the Kubelka–Munk function.²⁵

Results

The crystalline phase in the samples was identified as $\text{Bi}_{0.6}\text{Y}_{0.4}\text{O}_{1.5}$ (cubic, $a \approx 0.545$ nm) by powder X-ray diffraction. Table 1 shows the excess oxygen content, δ , in the specimens, $\text{Bi}_{0.6}\text{Y}_{0.4}\text{O}_{1.5+\delta}$, prepared under different atmospheres. The δ values obtained by titration corresponded to those obtained from TG; values of δ increased with increasing oxygen partial pressure. The sample with the smallest value of δ of zero was obtained under nitrogen; that with largest value of δ of 0.16 was obtained under the HIP condition.

The anion-deficient fluorite structure was retained in the region $0 \leq \delta \leq 0.16$, as shown in Fig. 1(a). However, the lattice

Table 1 Excess oxygen content δ of samples annealed at 703 K as determined by iodometric titration and thermogravimetry

sample	atmosphere	δ	colour
1	N_2 (1 atm)	0	lemon yellow
2	air	0.01	orange
3	O_2 (20 atm)	0.07	red–brown
4	Ar–O_2 (4:1) (1500 atm)	0.16	black–brown

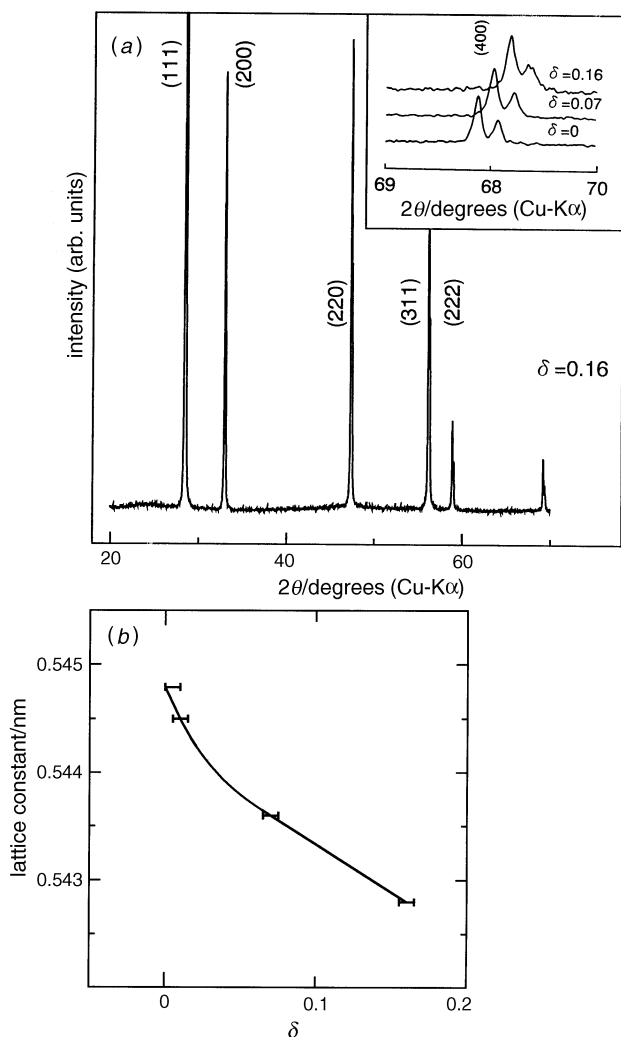


Fig. 1 (a) X-Ray powder diffraction patterns of $\text{Bi}_{0.6}\text{Y}_{0.4}\text{O}_{1.5+\delta}$ with $\delta = 0, 0.07$ and 0.16 . Diffraction peaks were indexed on the assumption of a fluorite structure. The inset is an enlargement of the (400) diffraction. (b) Cubic lattice constants for $\text{Bi}_{0.6}\text{Y}_{0.4}\text{O}_{1.5+\delta}$ as a function of the excess oxygen content, δ .

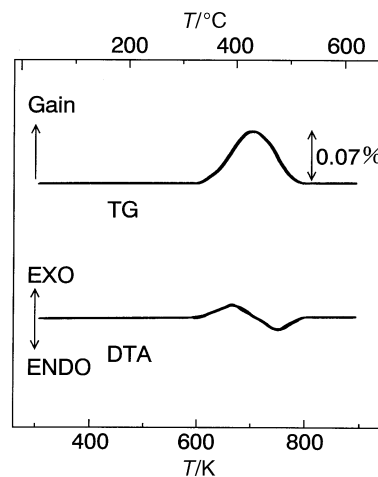


Fig. 2 TG–DTA curves of $\text{Bi}_{0.6}\text{Y}_{0.4}\text{O}_{1.50}$ ($\delta = 0$) as a starting sample. The measurements were carried out under O_2 gas flow.

constant decreased with increasing δ [Fig. 1(b)], as evidenced by the shift of the (400) diffraction peak in the inset in Fig. 1(a). Simultaneously an increase in the full width at half maximum at the peak was seen with increasing δ .

Fig. 2 shows TG and DTA traces for measurements carried out under an oxygen flow for $\text{Bi}_{0.6}\text{Y}_{0.4}\text{O}_{1.50}$ ($\delta = 0$) as the starting material. The TG curve showed an increase in mass up to 703 K and a decrease to the original mass at higher temperature, indicating that a high oxidation state was formed at *ca.* 703 K under oxygen flow and that the incorporated excess oxygen was released at higher temperature. In accord with the increase and decrease in mass, exothermic and endothermic peaks were observed in the DTA trace, respectively.

The temperature dependence of the dc electrical conductivity of $\text{Bi}_{0.6}\text{Y}_{0.4}\text{O}_{1.66}$ was measured in the temperature range 573–400 K, where significant change in δ did not occur during the measurement. Semiconductive and thermal activation type behaviour with an activation energy of 0.9 eV was observed. The conductivity at 500 K was $1 \times 10^{-7} \text{ S cm}^{-1}$. $\text{Bi}_{0.6}\text{Y}_{0.4}\text{O}_{1.50}$ also showed similar conductivities.

The colours of the sintered discs changed from lemon yellow for $\delta = 0$ through orange for $\delta = 0.01$, brown for $\delta = 0.07$, and finally to black–brown for $\delta = 0.16$. Fig. 3 shows the optical absorption spectra for samples $\text{Bi}_{0.6}\text{Y}_{0.4}\text{O}_{1.5+\delta}$ and the inset shows the dependence of the absorption edge on δ . The edge in each spectrum was estimated from an intersection point

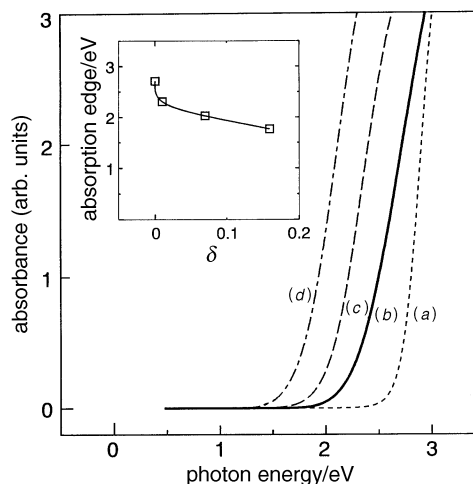


Fig. 3 Optical absorptions of $\text{Bi}_{0.6}\text{Y}_{0.4}\text{O}_{1.5+\delta}$ [(a) $\delta = 0$, (b) $\delta = 0.01$, (c) $\delta = 0.07$, (d) $\delta = 0.16$]. Data were obtained by transforming from diffuse reflectivity spectra with the Kubelka–Munk function.²⁵ The inset shows absorption edges as a function of the excess oxygen content, δ .

between the x-axis and a straight line drawn from the higher energy side along the observed spectrum. It was noted that a decrease of *ca.* 1 eV in the energy of the absorption edge was observed upon changing δ from 0 to 0.16.

Discussion

Incorporation of excess oxygen

It should be pointed out that excess oxygen is introduced even under moderate conditions. The dependence of lattice constant on δ in Fig. 1(b) indicates that the excess oxygen is incorporated continuously into the crystal lattice, although the anionic positions could not be determined by the powder X-ray diffraction method owing to the weakly scattering nature of oxygen atoms in these oxides. The increase in the full width at half maximum of the diffraction peak with increasing δ [Fig. 1(a)] indicates a decrease of the crystalline size. The TG-DTA traces in Fig. 2 show that the excess oxygen is introduced easily up to the composition of $\text{Bi}_{0.6}\text{Y}_{0.4}\text{O}_{1.51}$, calculated from the maximum in the mass gain at 703 K. A high oxidation state was formed at *ca.* 703 K under oxygen flow and the incorporated excess oxygen was released at higher temperature.

Mixed-valence state of Bi

We propose the formation of a mixed-valence state, $\text{Bi}^{3+}\text{--Bi}^{5+}$, which can explain consistently the observed phenomena discussed above. The results of iodometric titrations indicate the oxidation of Bi^{3+} because Y^{3+} is known only to adopt the trivalent state. Using this assumption, the $\text{Bi}^{5+}/(\text{Bi}^{3+} + \text{Bi}^{5+})$ ratio in $\text{Bi}_{0.6}\text{Y}_{0.4}\text{O}_{1.66}$ is 0.27. The low conductivities observed for the sample with $\delta=0.16$ ruled out the possibility of the formation of the single-valence state, $\text{Bi}^{3.53+}$, or that of mobile positive holes. Therefore, disproportionation of Bi ions is expected. The lattice contraction shown in Fig. 1(b) originates from the formation of Bi^{5+} whose ionic radius is smaller than that of Bi^{3+} , even though excess oxygen is introduced into the lattice. The two types of Bi ion must adopt different chemical environments. However, site distinction was impossible in the X-ray powder diffraction patterns, owing to the similar scattering nature of Bi^{3+} and Bi^{5+} in these oxides.

It is well known that excess oxygen often leads to the formation of positive holes in the valence band in semiconductive ionic compounds.^{26,27} However, positive holes in the valence band composed of $\text{Bi}^{3+} 6s^2$ orbitals in semiconductive oxides have not, to our knowledge, been reported. In the present experiments, two holes caused by excess oxygen are trapped on Bi^{3+} , resulting in the formation of Bi^{5+} . Such newly formed Bi^{5+} is expected to attract O^{2-} more than Bi^{3+} , owing to the large positive charge. This lattice relaxation annihilating the holes might originate from the softness of the ionic lattice containing Bi^{3+} . Battle *et al.* concluded from neutron scattering measurements and NMR spectra that there is local ordering of anion vacancies depending on adjacent cationic species.^{20–22} It is reasonable to consider that the introduction of excess oxygen increases the amount of lattice defects, since newly formed Bi^{5+} can be regarded as a defect. The large polarizability of Bi^{3+} , with $6s^2$ electrons, may result in disorder of the three types of cations, Bi^{3+} , Y^{3+} , and Bi^{5+} , which prefer different local structures.

Optical absorption

Finally, we consider the origin of the observed red shift with increase in δ in the optical absorption spectra in Fig. 3; such an observation in these solid oxides has not been previously reported. The formation of Bi^{5+} has a large influence on the optical absorption edge in $\text{Bi}_{0.6}\text{Y}_{0.4}\text{O}_{1.5+\delta}$. Fig. 4 shows the proposed schematic energy band diagram of $\text{Bi}_{0.6}\text{Y}_{0.4}\text{O}_{1.50}$ and

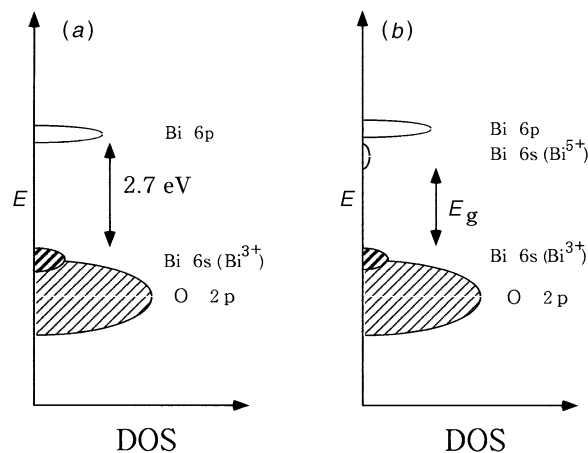


Fig. 4 Schematic energy band diagram of $\text{Bi}_{0.6}\text{Y}_{0.4}\text{O}_{1.5+\delta}$ with (a) $\delta=0$ and (b) $\delta\approx 0.16$

$\text{Bi}_{0.6}\text{Y}_{0.4}\text{O}_{1.5+\delta}$ ($\delta\approx 0.16$). For $\delta>0$, the $6s^0$ state of Bi^{5+} is expected to lie just below the conduction band. As δ increases, the level of the $6s^0$ state shifts to lower energy and the bottom of the conduction band may start to be composed of $\text{Bi}^{5+} 6s^0$. The origin of the gap-narrowing seems to be the appearance of unoccupied Bi $6s^0$ below the Bi $6p^0$ conduction band. Therefore, the observed optical absorption at lower energy is due to the intervalence charge-transfer absorption from $\text{Bi}^{3+} 6s^2$ to $\text{Bi}^{5+} 6s^0$. The transition might be caused by the direct interaction between Bi^{3+} and Bi^{5+} as a consequence of the short distance, *ca.* 0.384 nm, between each cation in the fluorite structure for $\text{Bi}_{1-x}\text{Y}_x\text{O}_{1.5+\delta}$.

Conclusions

Polycrystalline $\text{Bi}_{0.6}\text{Y}_{0.4}\text{O}_{1.5+\delta}$ was synthesized at 703 K by controlling the oxygen partial pressure. The results obtained are summarized below.

(1) A zero value of δ was obtained under nitrogen and the highest δ value, 0.16, under Ar--O_2 (4:1) (1500 atm). The anion-deficient fluorite structure was retained in the region $0\leq\delta\leq 0.16$, although the lattice constant decreased gradually with increasing δ .

(2) As δ increased, the colour of the samples changed from lemon yellow to black-brown and the bandgap E_g , estimated from the diffuse reflectance spectra, decreased from 2.7 to 1.7 eV. The temperature dependence of dc electrical conductivities of $\text{Bi}_{0.6}\text{Y}_{0.4}\text{O}_{1.66}$ and $\text{Bi}_{0.6}\text{Y}_{0.4}\text{O}_{1.50}$ measured under air in the temperature range 400–573 K showed Arrhenius type behaviour with an activation energy of 0.9 eV.

(3) The change of optical absorption was explained in terms of the formation of the mixed-valence state $\text{Bi}^{3+}\text{--Bi}^{5+}$.

The authors wish to thank Dr. T. Hayashi and Dr. Y. Awakura of the Shonan Institute of Technology for help with the use of the HIP. They are grateful to the staff of UVSOR of the Institute for Molecular Science. One of the authors (H. M.) thanks the Japan Society for the Promotion of Science. The work was supported in part by a Grant-in-Aid for Scientific Research from the Ministry of Education, Science, Sports, and Culture, Japan.

References

- 1 M. B. Robin and P. Day, *Adv. Inorg. Chem. Radiochem.*, 1967, **10**, 247.
- 2 P. Day, *Int. Rev. Phys. Chem.*, 1981, **1**, 149.
- 3 P. Day, *Inorg. Chem.*, 1963, **2**, 452.
- 4 A. W. Sleight, J. L. Gillson and P. E. Bierstad, *Solid State Commun.*, 1975, **17**, 27.

- 5 T. Nakamura, S. Kose and T. Sata, *J. Phys. Soc. Jpn.*, 1971, **31**, 1284.
- 6 M. Jansen, *Z. Naturforsch., Teil B*, 1977, **32**, 1340.
- 7 G. Gatlow and W. Klippel, *Z. Anorg. Allg. Chem.*, 1980, **470**, 25.
- 8 J. Trehoux, F. Abraham, D. Thomas, C. Doremieux-Morin and H. Arribart, *J. Solid State Chem.*, 1988, **73**, 80.
- 9 R. A. Beyerlein, A. J. Jacobson and K. R. Poeppelmeier, *J. Chem. Soc., Chem. Commun.*, 1988, 225.
- 10 B. Begemann and M. Jansen, *J. Less-Common Met.*, 1989, **156**, 123.
- 11 S. Uma and J. Gopalakrishnan, *J. Solid State Chem.*, 1993, **153**, 595.
- 12 J. Pannetier, D. Tranqui and A. W. Sleight, *Mater. Res. Bull.*, 1993, **28**, 989.
- 13 K. P. Reis, A. J. Jacobson and J. Kulik, *Chem. Mater.*, 1993, **5**, 1070.
- 14 N. Kinomura and N. Kumada, *Mater. Res. Bull.*, 1995, **30**, 129.
- 15 N. Kumada, N. Kinomura, P. M. Woodward and A. W. Sleight, *J. Solid State Chem.*, 1995, **116**, 281.
- 16 H. Mizoguchi, H. Kawazoe, T. Ueda, S. Hayashi, H. Hosono and N. Ueda, *Bull. Chem. Soc. Jpn.*, 1996, **69**, 111.
- 17 T. Takahashi, H. Iwahara, and T. Arao, *J. Appl. Electrochem.*, 1975, **5**, 187.
- 18 T. Takahashi, T. Esaka, and H. Iwahara, *J. Appl. Electrochem.*, 1977, **7**, 299.
- 19 P. D. Battle, C. R. A. Catlow, J. Drennan and A. D. Murray, *J. Phys. C: Solid State Phys.*, 1983, **16**, L561.
- 20 P. D. Battle, C. R. A. Catlow, J. W. Heap and L. M. Moroney, *J. Solid State Chem.*, 1986, **63**, 8.
- 21 P. D. Battle, C. R. A. Catlow, A. V. Chadwick, P. Cox, G. N. Greaves and L. M. Moroney, *J. Solid State Chem.*, 1987, **69**, 230.
- 22 P. D. Battle, B. Montez and E. Oldfield, *J. Chem. Soc., Chem. Commun.*, 1988, 584.
- 23 H. Kruidhof, K. J. de Vries and A. J. Burggraaf, *Solid State Ionics*, 1990, **37**, 213.
- 24 H. Kruidhof, H. J. M. Bouwmeester, J. de Vries, P. J. Gellings and A. J. Burggraaf, *Solid State Ionics*, 1992, **50**, 181.
- 25 P. Kubelka and F. Munk, *Z. Technol. Phys.*, 1931, **12**, 593.
- 26 N. M. Tallan and R. W. Vest, *J. Am. Ceram. Soc.*, 1966, **49**, 401.
- 27 M. F. Lasker and R. A. Rapp, *Z. Phys. Chem.*, 1966, **49**, 198.

Paper 6/08504K; Received 19th December, 1996